

## Solubilization of Acyl Heterogeneous Triacylglycerol in Phosphatidylcholine Vesicles

RONG LI,<sup>†</sup> WALTER SCHMIDT,<sup>‡</sup> SCOTT RANKIN,<sup>§</sup> ROSEMARY L. WALZEM,<sup>#</sup> AND ELIZABETH BOYLE-RODEN<sup>\*,†</sup>

Department of Nutrition and Food Science, University of Maryland, College Park, Maryland 20742, Nuclear Magnetic Resonance Facility, Environmental Quality Laboratory, U.S. Department of Agriculture, Agricultural Research Service, Beltsville, Maryland 20705, Department of Food Science, University of Wisconsin, Madison, Wisconsin 53706, and Department of Poultry Science, Texas A&M University, College Station, Texas 77843

The amount of acyl heterogeneous triacylglycerol (TG<sub>HET</sub>) solubilized by phosphatidylcholine (PC) vesicles, prepared by co-sonication of egg PC and small amounts (<6% w/w) of TG<sub>HET</sub>, was determined using <sup>13</sup>C nuclear magnetic resonance (NMR). The acyl chains of TG<sub>HET</sub> were predominantly 16 or 18 carbons in length, 50% saturated, and approximately 21.7% <sup>13</sup>C isotopically enriched at the carbonyl carbon. The <sup>13</sup>C NMR spectra revealed two carbonyl resonances at chemical shift values between PC carbonyls and oil-phase TG carbonyls, confirming the presence of TG<sub>HET</sub> solubilized in PC vesicles. Oil-phase TG carbonyl peaks were present only in spectra of vesicles containing >3 wt % TG<sub>HET</sub>. Integration of TG<sub>HET</sub> carbonyl resonances determined that PC vesicles solubilized 3.8 wt % of TG<sub>HET</sub>, compared to 2.8 wt % of acyl homogeneous triolein. The difference between the maximum solubility of TG<sub>HET</sub> and that of homogeneous TG (TG<sub>HOM</sub>) with similar acyl chain lengths provides evidence that specific acyl composition, in addition to the acyl chain length of triacylglycerols, affects the solubility of TG in PC vesicles and TG-rich lipoprotein surfaces. Thus, TG<sub>HET</sub> may innately be a better model substrate than TG<sub>HOM</sub> for determination of substrate availability of TG at lipoprotein surfaces.

**KEYWORDS:** Solubilization; heterogeneous; triacylglycerol; vesicle; <sup>13</sup>C nuclear magnetic resonance

### INTRODUCTION

Long-chain triacylglycerols (TG) are the main storage form of energy in most animals. They are transported in the circulation as components of TG-rich lipoprotein particles. TG are hydrophobic molecules and thus are primarily located within the core of TG-rich lipoprotein particles and stabilized by an emulsifying layer of phospholipid, cholesterol, and apolipoproteins. However, key enzymes regulating the metabolism of TG via hydrolysis or transfer are predominantly located in the aqueous medium surrounding lipoprotein particles. Lipases and transfer proteins presumably access the small but finite amount (2–5 wt %) of TG in the lipoprotein surface monolayer, as indicated by phase equilibrium studies (*1*). In phosphatidylcholine (PC) bilayers, 2.8 wt % of triolein (TO) is solubilized in an orientation appropriate for enzymatic hydrolysis (*1*). In general, the solubility of TG in PC bilayers increases as TG acyl chain length decreases (*1–4*). Additionally,

the presence of cholesterol, cholesterol esters, or other acylglycerols variably reduces the solubility of TG in PC vesicles (*1, 3–9*). However, all previous measurements of TG in a phospholipid surface of intact particles have been made using acyl homogeneous TG such as triolein or tripalmitin. Under standard physiological conditions, very little of the TG present in TG-rich lipoproteins would be acyl homogeneous. Direct measurements of the surface solubility of the more physiologically relevant acyl heterogeneous TG (TG<sub>HET</sub>) have not been made because, until recently, acyl heterogeneous TG isotopically enriched with <sup>13</sup>C at the carbonyl carbon have not been available. The direct measurement of surface-located TG in intact particles can be made only using <sup>13</sup>C nuclear magnetic resonance (NMR) and <sup>13</sup>C-carbonyl-enriched TG. Thus, the primary objective of this study was to measure the solubility of TG<sub>HET</sub> in PC vesicles and compare this to values of acyl homogeneous TG.

The results provide data on the surface solubility and thus the substrate availability of physiologically relevant TG molecules. The regulation of TG metabolism is critical to overall energy balance. Information regarding the surface availability of TG in lipoprotein particles is essential to an improved understanding of TG-rich lipoprotein metabolism.

\* Corresponding author. Current address: 12429 Teal Ln., Pickerington, OH 43147.

<sup>†</sup> University of Maryland.

<sup>‡</sup> U.S. Department of Agriculture.

<sup>§</sup> University of Wisconsin.

<sup>#</sup> Texas A&M University.

## MATERIALS AND METHODS

**Materials.**  $^{13}\text{C}$ -carbonyl-enriched acyl heterogeneous TG were obtained from the liver of roosters fed a combination of  $^{13}\text{C}_3$ -(1,1,1)-trioleoylglycerol and  $^{13}\text{C}_1$ -palmitate (Boyle-Roden and Walzem, personal communication). Triolein, Trizma hydrochloride, and Trizma base were purchased from Sigma Chemical Co. (St. Louis, MO). Phosphatidylcholine was purchased from Avanti Polar Lipids (Alabaster, AL). Lipid standards, TLC 18-4A and GC 68A, and heptadecenoic acid were purchased from Nuchek (Elysian, MN). Methyl tridecanoate and  $\text{D}_2\text{O}$  (99.9%) were purchased from Aldrich Chemical Co. (Milwaukee, WI). Normal-phase TLC plates were purchased from Whatman (Clifton, NJ). Normal-phase Sep-Pak columns were purchased from Waters (Milford, MA). All other chemicals used were reagent grade.

**Lipid Extraction.** Lipids were extracted from rooster liver using a procedure documented by Christie (10). The extracted lipids were transferred to a 500-mL round-bottom flask and evaporated to dryness using a rotary evaporator (Buchi RE111, Switzerland) in a 50 °C water bath. Lipids were redissolved in 30–40 mL of benzene and transferred to preweighed vials, the solvent was evaporated under nitrogen ( $\text{N}_2$ ), and dried lipids were weighed.

Lipids were separated by column chromatography (11). Approximately 60 mg of total lipids was dissolved in 0.5 mL of benzene/hexane (1:1 v/v), applied to a 2-g silica Sep-Pak column, and sequentially washed with 30 mL each of benzene/hexane (1:1 v/v), benzene, benzene/ethyl ether (9:1 v/v), and ethyl ether, followed by 50 mL of methanol. Eluants were collected in 5-mL fractions and analyzed for lipid content by thin-layer chromatography (TLC). Alternatively, 150 mg of total lipids was applied to a 5-g silica Sep-Pak column and sequentially washed with 80 mL each of the solvents listed above with the same sequence, followed by 150 mL of methanol, with eluants collected in 10-mL fractions.

Each fraction was concentrated to 1 mL under  $\text{N}_2$ , and 10  $\mu\text{L}$  was spotted to TLC plates. Lipid classes were separated and identified by comparison to authentic lipid standards following the methods of Christie (12). Briefly, 10–20  $\mu\text{L}$  of each eluant fraction and 10  $\mu\text{g}$  each of lipid standards were applied to TLC plates (silica gel 60A, 250  $\mu\text{m}$  thickness), separated with a mobile phase of hexane/ethyl ether/formic acid (80:20:2 v/v), and visualized with iodine vapors or 50% (v/v) sulfuric acid. Duplicate plates without sulfuric acid or iodine vapor were prepared and visualized with 2',7'-dichlorofluorescein to allow for quantitative analysis of lipid by gas chromatography (GC) (13).

**FFA Profile and  $^{13}\text{C}$  Enrichment Ratio—GC-MS Spectrometry.** Lipid bands scraped from TLC plates were extracted with 1 mL of benzene. Twenty micrograms of heptadecenoic acid (C17:1) was added as the internal standard. Hydrolyzation and methylation of the extracted lipids were done by holding the mixture in a 60 °C water bath for 2 h with 3 mL of acetyl chloride/methanol (1:15). Ten micrograms of methyl tridecanoate (C13:0) was added as an internal standard, and 1 mL of water was added to break the emulsion. The top layer, containing fatty acid methyl esters (FAMES) in benzene, was aspirated to GC vial inserts. Retention times for specific FAMES were identified by comparison with authentic fatty acid methyl ester standards (GLC mixture 68A, Nuchek prep., Elysian, MN).

One microliter of FAMES, prepared as described, was separated and identified using a Hewlett-Packard 6890 series GC equipped with an Rtx-2330 30.0-m  $\times$  250- $\mu\text{m}$   $\times$  0.2- $\mu\text{m}$  column (Restek, Bellefonte, PA) and a HP 5973 mass-selective detector. Peaks were identified with the NIST Mass Library Spectra Database. The average  $^{13}\text{C}$  enrichments for  $\text{TG}_{\text{HET}}$  acyl chains were calculated using eq 1,

$$\frac{(M + 1)}{M} - \text{natural enrichment ratio} \quad (1)$$

where  $M$  is the abundance of the parent molecular ion,  $M + 1$  is the abundance of the isotopic ion with one additional mass number; and the natural enrichment ratio was calculated as the total natural abundance isotopic enrichment ratio of all atoms in the molecule (14).

**Table 1.** Lipid Composition of PC Vesicles Containing 1–6 Wt %  $^{13}\text{C}$ - $\text{TG}_{\text{HET}}$ <sup>a</sup>

lipid	lipid weight (mg)						
	1 wt % sample	2 wt % sample	2.5 wt % sample	3 wt % sample	4 wt % sample	5 wt % sample	6 wt % sample
$^{13}\text{C}_3$ - $\text{TG}_{\text{HET}}$	0.50	1.00	1.25	1.50	2.00	2.50	3.00
EYPC	49.50	49.00	48.75	48.50	48.00	47.50	47.00

<sup>a</sup> All samples were prepared in duplicate except for the 6 wt %  $\text{TG}_{\text{HET}}$ , which was a single preparation.

**Vesicle Preparation.** Appropriate amounts of lipids (Table 1) were transferred from stock solutions of extracted liver TG, combined in a 7-mL vial, vortexed, and dried to a thin lipid film under  $\text{N}_2$ . Lipids were dissolved in 2 mL of 0.01 M Tris containing 0.1 M NaCl and 20%  $\text{D}_2\text{O}$  (v/v), pH 7.4, to form a 50 mg/mL solution and sonicated for 40–60 min in pulse mode with 10-s cycles (Sonic Dismembrator, Fisher Scientific, Pittsburgh, PA).

**Particle Size Analysis.** Small aliquots (5–10  $\mu\text{L}$ ) of the vesicles were placed in a small glass cuvette, which contained 0.7 mL of distilled water. The cuvette was inserted in the PSS NICOMP Submicron Particle Analyzer (Santa Barbara, CA) to yield an intensity of 300–600 kHz. Particles were sized by dynamic laser light scattering in vesicle mode and automatically analyzed, and the particle size distribution is presented as particle diameter, in nanometers, on a number weight basis (15).

**$^{13}\text{C}$  Nuclear Magnetic Resonance Spectroscopy.**  $^{13}\text{C}$  NMR spectra were acquired on an AM400 MHz Bruker NMR spectrometer. Acquisition parameters were as follow: sweep width, 20 kHz; 16K points; 60° excitation pulse (6.6  $\mu\text{s}$ ); acquisition delay at 2.2 s; acquisition time, 0.3 s; 20 000 scans. The magnetic homogeneity of each sample was monitored before and after  $^{13}\text{C}$  spectra were obtained by determining the line width at half-height ( $\nu_{1/2}$ ) of the water peak from a  $^1\text{H}$  spectra of a single acquisition (sweep width, 3000 Hz; 8K points). FID were processed with automatic baseline correction, exponential line broadening of 3 Hz, Fourier transformation, and automatic phasing. Chemical shift values were referenced to the terminal methyl carbon at 14.10 ppm (1). Chemical shift values and integration of peak areas were measured digitally, and line width values were determined automatically using Lorentzian fit by MacFID Software v. 5.2 (Tecmag, Houston, TX).

The longitudinal relaxation time ( $T_1$ ) was measured according to the methods of Vold et al. (16) using a 300-MHz GE NMR spectrometer equipped with a heteronuclear 5-mm  $^1\text{H}/^{13}\text{C}$  probe at 25 °C.

**Calculation of TG Solubility in PC Vesicles.** The amount of TG solubilized by PC vesicles was determined by two methods: (1) plotting the sums of integrals of TG carbonyls (Figure 2, below) and (2) comparing the ratio of PC and TG carbonyls. For plotting, the sums of the integrals of TG carbonyls solubilized by PC were plotted on the y-axis versus the weight % compositions of TG used to prepare vesicles on the x-axis. Additionally, the sums of the integrals of TG carbonyls in the oil phase were plotted against the weight % compositions of TG used to prepare vesicles. The x-intercept of the regression line for the oil-phase carbonyls and the break point in the regression line of the surface-phase carbonyls were averaged to determine the weight % solubility of TG in PC vesicles.

TG solubility was also calculated by comparison of the PC carbonyls to the surface-phase TG carbonyls. The expected, or theoretical, ratio of the intensity of PC carbonyls to TG carbonyls in the NMR spectrum was calculated using the mass and  $^{13}\text{C}$  enrichment levels of PC and TG (1, 15) (Tables 1 and 2). The theoretical PC:TG carbonyl integral ratio is derived from the known lipid composition of the vesicles and is given in eq 2. The empirical PC:TG carbonyl ratio is determined from the NMR spectra using the integrals of the phospholipid and TG carbonyl peaks in eqs 3–5. Area ratios of surface TG:PC reached a plateau when the original TG contents were 4 and 5 wt %. The average of these two ratios was utilized to estimate the total TG content in the original solution by calculating  $x$  in eq 2, where  $x$  is the amount of TG in the vesicles. The calculated values match known input weights well.

**Table 2.** Fatty Acid Profile, Average Molecular Weight, and <sup>13</sup>C Enrichment of TG<sub>HET</sub> Recovered from Plasma and Liver

fatty acid	fatty acid profile (mol %) <sup>a</sup>		% <sup>13</sup> C isotopic enrichment <sup>b</sup>	
	plasma	liver	plasma	liver
C14:0	0.5	0.5	1.5	
C15:0	0.3	0.6		1.1
C16:0	19.8	36.8	30.1	14.3
C16:1	1.4	1.7		6.0
C18:0	5.3	11.3		4.7
C18:1	54.0	43.1	50.7	36.6
C18:2	16.4	5.7	0.2	
C18:3	1.1	0.2	20.7	0.5
C20:0		0.1		
C20:1				
C20:3	0.4			
C20:4	0.8	0.1		
C22:0				
C24:1				
S/U <sup>c</sup>	0.4	1		
MW average	866.5	852.8		
<sup>13</sup> C isotopic enrichment weighted average			33.7	21.7

<sup>a</sup> Values are the averages of triplicate analyses. <sup>b</sup> Values are the averages of duplicate analyses. <sup>c</sup> Saturated-to-unsaturated ratio.

$$\frac{x \text{ mg TG} \times \frac{1}{852.8} \times 21.7(\% \text{ enrichment}) \times 3 \text{ carbonyls}}{(100 - x) \times \frac{1}{760.1} \times 1.1(\% \text{ enrichment}) \times 2 \text{ carbonyls}} \quad (2)$$

area ratio of total TG/PC =

$$\left( \int S_{1,3} + \int S_2 + \int O_{1,3} + \int O_2 \right) / \left( \int P_i + \int P_o \right) \quad (3)$$

$\int S_{1,3}$  is the integral of the resonance for the *sn*-1,3 TG carbonyls solubilized in the PC bilayer,  $\int S_2$  is the integral of the resonance for the *sn*-2 TG carbonyls solubilized in the PC bilayer,  $\int O_{1,3}$  is the integral of the resonance for the *sn*-1,3 TG carbonyls in the oil phase,  $\int O_2$  is the integral of the resonance for the *sn*-2 TG carbonyls in the oil phase,  $\int P_i$  is the integral of the resonance for the PC carbonyls on the inner bilayer leaflet, and  $\int P_o$  is the integral of the resonance for the PC carbonyls on the outer bilayer leaflet.

$$\text{area ratio of surface TG/PC} = \left( \int S_{1,3} + \int S_2 \right) / \left( \int P_i + \int P_o \right) \quad (4)$$

area ratio of surface TG/oil TG =

$$\left( \int S_{1,3} + \int S_2 \right) / \left( \int O_{1,3} + \int O_2 \right) \quad (5)$$

Area ratios of surface TG/PC plateaued when the original TG contents were >3 wt %. The average of these surface TG/PC ratios was then used to estimate the surface TG content in the vesicles by solving for *x* in eq 2.

The limitations and assumptions used to calculate the solubility of TG in PC vesicles included (1) the integration accuracy of the small PC and TG carbonyl peaks, (2) the assumption that TG carbonyls in the surface and core phases and PC carbonyls experience similar mechanisms and degree of relaxation during acquisition, and (3) the assumption that nuclear Overhauser effect (NOE) values of TG<sub>HET</sub> carbonyls in surface and core phases were equivalent to the corresponding NOE values for triolein. In addition, the calculation of TG solubility on the basis of TG/PC ratios included additional variability arising from calculations of the average <sup>13</sup>C enrichment and average molecular weight of TG<sub>HET</sub>.

**Statistical Analysis.** Duplicate integrals of TG carbonyls were calculated for averages and standard errors at various treatment levels. Simple linear regression analyses were conducted on sums of integrals of TG carbonyls solubilized in PC using all treatment levels (1–6% TG<sub>HET</sub>), 1–3% and 4–5% TG<sub>HET</sub>, and for sums of integrals of TG

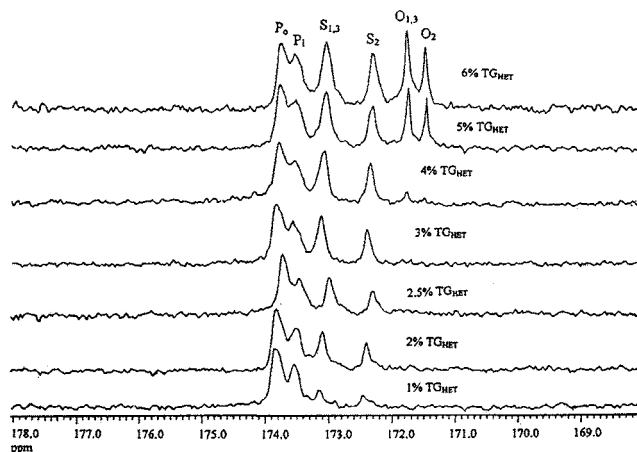


**Figure 1.** <sup>13</sup>C NMR spectra of the enlarged carbonyl region of PC vesicles containing from 1 to 6 wt % <sup>13</sup>C-enriched TG<sub>HET</sub>. P<sub>o</sub> and P<sub>i</sub> stand for inner and outer leaflet PL carbonyl carbons. Four peaks labeled S<sub>1,3</sub>, S<sub>2</sub>, O<sub>1,3</sub>, and O<sub>2</sub> are TG carbonyls. S<sub>1,3</sub> and S<sub>2</sub> are TGs solubilized in the PC bilayer, while O<sub>1,3</sub> and O<sub>2</sub> are TGs in the oil phase. 1, 2, and 3 indicate the *sn* positions of the specific carbonyl carbons.

carbonyls in the oil phase at 4–5% TG<sub>HET</sub>. The significance level was set at *p* < 0.05.

## RESULTS

**Quantification of Extracted TG<sub>HET</sub>.** Approximately 140 and 80 mg of <sup>13</sup>C-carbonyl-enriched TG<sub>HET</sub> was recovered from the livers and plasma, respectively, of roosters fed a combination of <sup>13</sup>C<sub>3</sub>-(1,1,1)-trioleoylglycerol and <sup>13</sup>C<sub>1</sub>-palmitate. PC vesicles containing TG<sub>HET</sub> were prepared exclusively from TG<sub>HET</sub> recovered from the livers.

**Lipid Characterization.** The fatty acid profile and <sup>13</sup>C enrichment of TG<sub>HET</sub> are presented in Table 2. Of the fatty acyl chains in TG<sub>HET</sub>, which contained <sup>13</sup>C isotopic enrichment, approximately three-quarters were unsaturated. The average <sup>13</sup>C enrichment for TG<sub>HET</sub> was 21.7%.

**Particle Size.** The particle size distribution of model vesicles was stable over time and consistent for all treatments. Typically, 96.9% of vesicles had diameters ranging from 19.2 to 25.4 nm with a SD of ≤4.4 nm, and <4% had a size between 44.7 and 96.9 nm with a SD of ≤10.2 nm. Vesicle diameters were stable for at least 15 d following NMR experiments when samples were stored at 4 °C.

**<sup>13</sup>C Nuclear Magnetic Resonance.** The <sup>13</sup>C NMR spectra of PC vesicles containing 1–6 wt % <sup>13</sup>C-TG<sub>HET</sub> are shown in Figure 1. PC vesicles with less than or equal to 3 wt % TG<sub>HET</sub> revealed four distinct carbonyl resonances arising from PL carbonyls from the inner (P<sub>i</sub>) and outer vesicle leaflets (P<sub>o</sub>), or TG carbonyls solubilized in the phospholipid bilayer (TG<sub>s</sub>). TG<sub>s</sub> carbonyls in the *sn*-1 and *sn*-3 positions (TG<sub>S1,3</sub>) were clearly distinguished from TG carbonyls in the *sn*-2 position (TG<sub>S2</sub>). <sup>13</sup>C NMR spectra of PC vesicles containing greater than or equal to 4 wt % TG<sub>HET</sub> had six carbonyl resonances. In addition to P<sub>i</sub>, P<sub>o</sub>, TG<sub>S1,3</sub>, and TG<sub>S2</sub>, TG carbonyls arising from both the *sn*-1,3 positions (TG<sub>O1,3</sub>) and the *sn*-2 position (TG<sub>O2</sub>) of TG in an oil-phase environment (TG<sub>o</sub>) were present. The chemical shift values and line width at half-height of carbonyl resonances for PC vesicles containing <sup>13</sup>C-TG<sub>HET</sub> are given in Tables 3 and 4. The T<sub>1</sub> values for PL and TG carbonyls in both surface and oil phases were calculated for PC vesicles containing 5 mol % TG<sub>HET</sub> and compared to published values for PC vesicles containing triolein in Table 5.



**Table 3.** Comparison of Chemical Shift Values<sup>a</sup> of Selected Resonances in <sup>13</sup>C NMR Spectra of PC Vesicles Containing TG<sub>HET</sub>

resonance	1 wt %	2 wt %	2.5 wt %	3 wt %	4 wt %	5 wt %	6 wt %
P <sub>0</sub>	173.85 <sup>b</sup>	173.84	173.83	173.80	173.81	173.81	173.81
P <sub>1</sub>	173.54	173.55	173.57	173.52	173.53	173.56	173.59
TG <sub>S1,3</sub>	173.16	173.11	173.07	173.13	173.11	173.12	173.09
TG <sub>S2</sub>	172.47	172.44	172.42	172.42	172.40	172.39	172.38
TG <sub>O1,3</sub>					171.82	171.82	171.82
TG <sub>O2</sub>					171.54	171.54	171.55

<sup>a</sup> Data shown are the averages of duplicate analyses, SD ≤ 0.06. <sup>b</sup> <sup>13</sup>C NMR spectra were acquired at 25 °C using a standard one-pulse sequence with a 60° excitation pulse (6.6 μs), acquisition delay of 2.2 s, total pulse repetition time of 2.5 s, 20 000 scans, sweep width 20 000 Hz, 16K points. Spectra were processed with automatic baseline correction, exponential line broadening of 3 Hz, Fourier transformation, and automatic phasing. Chemical shift values and integration of peak areas were measured digitally. Chemical shift values were referenced to the terminal methyl carbon at 14.10 ppm.

**Table 4.** Comparison of Line Width at Half-Height<sup>a</sup> of Selected Resonances in <sup>13</sup>C NMR Spectra of PC Vesicles Containing TG<sub>HET</sub>

resonance	1 wt %	2 wt %	2.5 wt %	3 wt %	4 wt %	5 wt %	6 wt %
TG <sub>S1,3</sub>	5.9 <sup>2</sup>	9.7	11.9	11.9	13.0	16.1	14.5
TG <sub>S2</sub>	5.1	7.0	11.1	9.6	9.6	12.5	12.0
TG <sub>O1,3</sub>					2.5	5.8	4.0
TG <sub>O2</sub>					1.3	4.6	4.5
terminal CH <sub>3</sub> -	10.8	10.2	10.1	10.7	10.9	10.7	11.0

<sup>a</sup> Data shown are the average of the duplicate analysis, SD ≤ 1.6. <sup>b</sup> <sup>13</sup>C NMR spectra were acquired at 25 °C using a standard one-pulse sequence with a 60° excitation pulse (6.6 μs), acquisition delay of 2.2 s, total pulse repetition time of 2.5 s, 20 000 scans, sweep width 20 000 Hz, 16K points. Spectra were processed with automatic baseline correction, exponential line broadening of 3 Hz, Fourier transformation, and automatic phasing. Chemical shift values and integration of peak areas were measured digitally.

**Table 5.** T<sub>1</sub> Values of Vesicle Carbonyls

resonance	T <sub>1</sub> <sup>a</sup> (s)	
	5 wt % TO <sup>b</sup>	5 mol % TG <sub>HET</sub>
P <sub>0</sub>	2.3	2.1 ± 0.1
P <sub>1</sub>	2.0	2.1 ± 0.4
TG <sub>S1,3</sub>	2.2	2.4 ± 0.5
TG <sub>S2</sub>	1.9	2.2 ± 0.3
TG <sub>O1,3</sub>	2.1	2.3 ± 0.1
TG <sub>O2</sub>	1.9	1.7 ± 0.3

<sup>a</sup> The longitudinal relaxation time (T<sub>1</sub>) was measured according to the methods of Vold et al. (16). Acquisition parameters were 90° excitation pulse (10.2 μs), 11 s total repetition time, 500–2000 scans, and τ values 10 u, 100 m, 1 s, 2.5 s, and 4 s. <sup>b</sup> From Hamilton and Small (7), SD ≤ ±10%.

**Calculation of TG Solubility in PC Vesicles.** The maximum solubility of TG<sub>HET</sub> in PC bilayers was determined by plotting the sum of integrals of TG carbonyls solubilized in PC or oil peak TG carbonyls against the wt % TG composition of vesicles (Figure 2) (I). The maximum solubility of TG<sub>HET</sub> in PC bilayers was also estimated by comparison of the ratios of PC to surface TG<sub>HET</sub> carbonyls in <sup>13</sup>C NMR spectra (Table 6).

**Statistical Results.** Means of sums of the integrals of two TG carbonyl peaks solubilized in PC at increasing TG<sub>HET</sub> treatment levels were found to be 9.9 × 10<sup>5</sup>, 1.4 × 10<sup>6</sup>, 2.0 × 10<sup>6</sup>, 2.2 × 10<sup>6</sup>, 2.8 × 10<sup>6</sup>, and 2.6 × 10<sup>6</sup> units<sup>2</sup>. Means of sums of the integrals of two TG carbonyl peaks in the oil phase were 0 for TG<sub>HET</sub> concentrations from 1 to 3 wt % and 2.9 × 10<sup>5</sup> and 1.5 × 10<sup>6</sup> units<sup>2</sup> for 4 and 5 wt % TG<sub>HET</sub>, respectively.

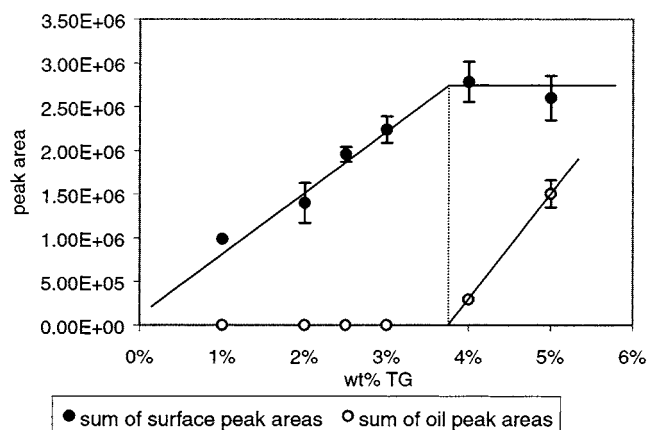


**Figure 2.** Plot of peak area of the surface and oil TG carbonyl peaks as a function of wt % TG<sub>HET</sub> in the starting mixture. Extrapolation of the oil peak regression line to the x-intercept yields the maximum solubility of TG<sub>HET</sub> in PC vesicles. In the case of surface peaks, regression lines were calculated before and after the appearance of oil peaks, and the intersection of the two surface peak regression lines was 3.8%, in agreement with the solubility limit predicted using the oil peak regression line.

**Table 6.** Ratio of Carbonyl Peak Areas in PC Vesicles Containing TG<sub>HET</sub>

composition	theoretical <sup>a</sup>	empirical <sup>b</sup>		
	TG/PC	TG/PC	TG <sub>S</sub> /TG <sub>O</sub>	
1 wt %	0.27	0.28	0.28	
2 wt %	0.53	0.38	0.38	
2.5 wt %	0.66	0.51	0.51	
3 wt %	0.80	0.61	0.61	
4 wt %	1.06	0.81	0.73	9.45
5 wt %	1.33	1.19	0.75	1.73
6 wt %	1.59	1.69	0.99	1.42

<sup>a</sup> Calculated from initial total lipid composition and the average isotopic <sup>13</sup>C-carbonyl enrichment and molecular weight of PC and TG<sub>HET</sub>. <sup>b</sup> Calculations were based on averaged integrals of duplicate measurements.

The R<sup>2</sup> values for regression lines of the sum of integrals of TG carbonyls solubilized in PC were 0.92, calculated using samples containing 1–3 wt % TG, and 0.83, calculated using all samples. Thus, regression analysis of the sum of the integrals of TG carbonyl peaks in the oil phase at 4 and 5 wt % TG<sub>HET</sub> concentrations was conducted separately, and the slope was found to be not significantly different from 0 (*p* = 0.52). The slope of the regression line calculated using the sum of integrals of TG carbonyls solubilized in PC from 1 to 3 wt % TG<sub>HET</sub> was significantly different from 0 (*p* = 0.0002, *y* = (6.4 × 10<sup>5</sup>)*x* + (2.8 × 10<sup>5</sup>), where *y* represents the integrals of surface TG while *x* represents the treatment TG concentrations). This line intersected the regression line of the sum of integrals of TG carbonyls solubilized in PC from 4 to 5 wt % TG<sub>HET</sub> at *x* = 3.8 wt %. At the same time, regression analysis on the sum of the integrals of TG carbonyls in the oil phase with 4–5% TG determined a line of *y* = (1.2 × 10<sup>6</sup>)*x* – (4.5 × 10<sup>6</sup>), where *y* is the oil-phase peaks' integral, while *x* is the wt % TG concentration; the slope was significantly different from 0 (*p* = 0.008). Extrapolation of the oil peak regression line to the *x*-intercept yields the maximum solubility of TG<sub>HET</sub> in PC vesicles. The intersection of the oil-phase peak line and the *x*-axis is 3.8 wt %. This value agrees very well with the intersection of surface TG regression lines (±0.001%).

## DISCUSSION

PC bilayers solubilize long-chain acyl heterogeneous TG to a greater extent than long-chain acyl homogeneous TG, such as triolein or tripalmitin. A maximum of 3.8 wt % TG<sub>HET</sub>, compared to 2.8 wt % triolein or 3.0 wt % tripalmitin, was solubilized in PC vesicles (1, 2). The chemical shift values, NOE values, and  $T_1$  relaxation times of carbonyl carbons in  $^{13}\text{C}$  NMR spectra of TG<sub>HET</sub> solubilized in PC vesicles did not vary significantly from respective values for triolein solubilized in PC vesicles (2), nor did PC vesicle diameters change with increasing amounts of TG<sub>HET</sub>; thus, vesicle size did not influence the surface solubility of TG<sub>HET</sub> between samples or compared to PC vesicles containing triolein.

The maximum solubility of TG<sub>HET</sub> in PC bilayers was determined by the secondary method of plotting the sum of integrals of TG carbonyls solubilized in PC or TG carbonyls in the oil phase against the wt % TG composition of vesicles (Figure 2) (1). The maximum solubility of TG<sub>HET</sub> in PC vesicles was estimated to be 2.8–2.9 wt % by calculation of the ratio of surface TG carbonyl peak areas to PC carbonyl peak areas in samples containing oil-phase TG. However, this method was considered to be less accurate due to the biological rather than synthetic nature of the TG<sub>HET</sub> used in this study and because no oil-phase TG<sub>HET</sub> peaks could be determined in duplicate  $^{13}\text{C}$  NMR spectra of PC vesicles containing 3 wt % TG<sub>HET</sub>. The calculation comparing PC carbonyl areas to surface TG carbonyl areas is dependent on both the molecular weight and the degree of  $^{13}\text{C}$ -carbonyl enrichment of TG<sub>HET</sub> and PC. The TG<sub>HET</sub> used in this study was obtained from a biological source and thus had a more variable content of isotopic  $^{13}\text{C}$ -carbonyl enrichment and had a calculated average molecular weight of 852.8, compared to the uniform 90% isotopic  $^{13}\text{C}$ -carbonyl enrichment and absolute molecular weight available for studies with triolein (1). The lower degree of isotopic  $^{13}\text{C}$  enrichment decreased the signal-to-noise of TG<sub>HET</sub> carbonyl peaks in  $^{13}\text{C}$  NMR spectra compared to published triolein  $^{13}\text{C}$  NMR spectra but did not affect the relative distribution of TG<sub>HET</sub> between surface and oil phases. However, the average  $^{13}\text{C}$  enrichment and molecular weights for TG<sub>HET</sub> did increase the variation and thus reduce the accuracy of calculated PC-to-TG<sub>HET</sub> carbonyl areas used to estimate surface TG<sub>HET</sub> solubility.

The primary differences between the TG<sub>HET</sub> used in this study and long-chain TG used to determine surface solubility in previous studies is the heterogeneous acyl composition. The TG<sub>HET</sub> contained 43% oleic and 37% palmitic acyl chains by weight, and the ratio of saturated acyl chains to unsaturated acyl chains was approximately 1:1. Thus, if length and general degree of saturation of TG acyl chains could predict surface solubility, the solubility of TG<sub>HET</sub> would presumably be intermediate between the solubilities of triolein and tripalmitin. However, TG<sub>HET</sub> also contained 5.7 wt % linoleic acid, and little data are available on the surface solubility of TG containing polyunsaturated acyl chains. One speculation is that TG<sub>HET</sub> may occupy greater molecular volume, as its three nonsimilar acyl chains could not align as closely as the acyl chains of triolein or tripalmitin when interspersed in the phospholipid interface. The presence of mono- and polyunsaturated acyl chains would increase the molecular volume occupied by each TG molecule. This greater molecular volume of TG<sub>HET</sub> may perturb the intermolecular packing of PC molecules in vesicles to a greater extent than either triolein or tripalmitin, creating more available space within the surface to be occupied by TG<sub>HET</sub>. Differential scanning calorimetry of neat samples of TG<sub>HET</sub> supports a more disordered molecular arrangement for TG<sub>HET</sub> compared to

triolein, as TG<sub>HET</sub> has a much lower phase transition temperature than triolein (Li, R.; Schmidt, W.; Boyle-Roden, E., unpublished).

The line width at half-height of NMR peaks may provide information on the mobility of the nuclei when spectra are acquired under similar conditions. It is interesting to note that the line width at half-height for surface TG<sub>HET</sub> increased with the wt % of TG<sub>HET</sub> (Table 4), indicating that TG<sub>HET</sub> was potentially more restricted within the surface as the total TG<sub>HET</sub> content increased. The line width at half-height of the terminal methyl ( $\text{CH}_3-$ ) was not appreciably affected by the increased concentration of TG<sub>HET</sub>.

The medium-chain acyl homogeneous TG, trioctanoin, is significantly more soluble in PC vesicles (10 mol %) than either triolein or TG<sub>HET</sub> (5). Thus, it appears that medium versus long acyl chain length of TG is more important than the heterogeneous versus homogeneous nature or extent of acyl chain unsaturation in determining the solubility of TG in phospholipid bilayers. It could be speculated that TG with mixed medium and long acyl chains, such as those found in dairy lipids, would be more soluble than the TG<sub>HET</sub> used in this study. The variation in the surface solubility of heterogeneous TG from distinct dietary sources such as butter versus soybean oil is unknown. However, as the rate of TG hydrolysis and TG transfer from lipoproteins may be affected by TG surface availability, it is interesting to speculate how the surface availability of TG may contribute to the variations in lipoprotein profiles or metabolism resulting from different dietary lipids.

In conclusion,  $^{13}\text{C}$  NMR spectra of TG<sub>HET</sub> in PC vesicles show that up to 3.8% of TG<sub>HET</sub> can be incorporated into the phospholipid bilayer. TG with a heterogeneous acyl composition of long chains are more soluble in PC bilayers than TG of similar chain length but homogeneous acyl content. This implies that more total TG may be available in the surface of TG-rich lipoproteins than predicted by models using triolein or tripalmitin alone.

## ABBREVIATIONS USED

EYPC, egg yolk phosphatidylcholine; FAME, fatty acid methyl ester; FFA, free fatty acid; GC, gas chromatography; HET, heterogeneous; HOM, homogeneous;  $T_1$ , longitudinal relaxation time; NMR, nuclear magnetic resonance; NOE, nuclear overhauser effect; PC, phosphatidylcholine; TLC, thin-layer chromatography; TG, triacylglycerol; TO, triolein.

## LITERATURE CITED

- (1) Hamilton, J. A.; Small, D. M. Solubilization and Localization of Triolein in Phosphatidylcholine Bilayers: A  $^{13}\text{C}$  NMR Study. *Proc. Natl. Acad. Sci. U.S.A.* **1981**, *78*, 6878–6882.
- (2) Hamilton, J. A. Interactions of Triacylglycerols with Phospholipids: Incorporation into the Bilayer Structure and Formation of Emulsions. *Biochemistry* **1989**, *28*, 2514–2520.
- (3) Hamilton, J. A.; Vural J. M.; Carpentier Y. A.; Deckelbaum R. J. Incorporation of Medium Chain Triacylglycerols into phospholipid bilayers: effect of long chain triacylglycerols, cholesterol, and cholesteryl esters. *J. Lipid Res.* **1996**, *37*, 773–782.
- (4) Deckelbaum, R. J.; Hamilton, J. A.; Moser, A.; Bengtsson-Olivecrona, G.; Butbul, E.; Carpentier, Y. A.; Gutman, A.; Olivecrona, T. Medium-Chain versus Long-Chain Triacylglycerol Emulsion Hydrolysis by Lipoprotein Lipase and Hepatic Lipase: Implications for the Mechanisms of Lipase Action. *Biochemistry* **1990**, *29*, 1136–1142.
- (5) Hamilton, J. A.; Miller K. W. Solubilization of Triolein and Cholesteryl Oleate in Egg Phosphatidylcholine Vesicles. *J. Biol. Chem.* **1983**, *258*, 12821–12826.

- (6) Spooner, P. J. R.; Small, D. M. Effect of Free Cholesterol on Incorporation of Triolein in Phospholipid Bilayers. *Biochemistry* **1987**, *26*, 5820–5825.
- (7) Miller, K. W.; Small, D. M. Surface-to-Core and Interparticle Equilibrium Distributions of Triacylglycerol-rich lipoprotein Lipids. *J. Biol. Chem.* **1983**, *258*, 13772–13784.
- (8) Miller, K. W.; Small, D. M. Triolein-Cholesteryl Oleate-Cholesterol-Lecithin Emulsions: Structural Models of Triacylglycerol-Rich Lipoproteins. *Biochemistry* **1983**, *22*, 443–451.
- (9) Miller, K. W.; Small, D. M. Structure of Triacylglycerol-rich Lipoproteins: an Analysis of Core and Surface Phases. In *Plasma Lipoproteins*; Elsevier: Amsterdam, 1987; pp 1–72.
- (10) Christie, W. W. Isolation, Separation, Identification and Structural Analysis of Lipids. In *Lipid Analysis*; Pergamon Press: Oxford, 1982; pp 17–23.
- (11) Horwitz, W. *Official Methods of Analysis of the Association of Official Analytical Chemists*, 12th ed.; Association of Official Analytical Chemists: Washington, DC, 1975; pp 515–516.
- (12) Christie, W. W. Isolation, Separation, Identification and Structural Analysis of Lipids. In *Lipid Analysis*; Pergamon Press: Oxford, 1982; pp 93–94.
- (13) Lyubachevskaya, G.; Boyle-Roden, E. Kinetics of 2-monoglyceride acyl migration in model chylomicra. *Lipids* **2000**, *35*, 1353–1358.
- (14) Lambert, J. B.; Shurvell, H. F.; Lightner D. A.; Cooks R. G. *Organic Structural Spectroscopy*; Prentice-Hall: Upper Saddle River, NJ, 1998; p 26.
- (15) Boyle, E.; Khan, M. A. Quantitative Analysis of Surface-Located Triacylglycerol in Intact Emulsion Particles. *J. Agric. Food Chem.* **2001**, *49*, 2014–2021.
- (16) Vold, R. L.; Waugh, J. S.; Klein, M. P.; Phelps, D. E. Measurement of Spin Relaxation in Complex Systems. *J. Chem. Phys.* **1968**, *48*, 3831–3832.

---

Received for review May 15, 2002. Revised manuscript received October 28, 2002. Accepted October 29, 2002.

JF025676N